Cement and Concrete Composites 96 (2019) 274–283

Contents lists available at ScienceDirect

Cement and Concrete Composites

journal homepage: www.elsevier.com/locate/cemconcomp

Effect of animal glue on mineralogy, strength and weathering resistance of calcium sulfate-based composite materials

Kerstin Elert*, Cristina Benavides-Reyes, Carolina Cardell

Department of Mineralogy and Petrology, Faculty of Science, University of Granada, Avenida Fuentenueva s/n, 18071, Granada, Spain

ARTICLE INFO

Keywords:
Gypsum
Bassanite
Anhydrite
Flexural strength
Compressive strength

ABSTRACT

Calcium sulfate (gypsum, bassanite, and anhydrite) has been widely used since ancient times as decorative plaster and painting grounds, often mixed with organic additives (e.g., animal glue). In order to evaluate the effect of organic additives on gypsum setting and on the product's final properties, calcium sulfate-based plaster samples, with and without the addition of animal glue, were subjected to accelerated weathering and mechanical testing. Test results were related to the samples' mineralogical composition. Animal glue improved mechanical properties and weathering resistance, but retarded gypsum setting and resulted in long-term stabilization of metastable bassanite and anhydrite. Accelerated weathering (wetting/drying cycles) resulted in changes in mineral phases and micro-texture, affecting mechanical properties and facilitating deterioration due to phase transition-related volume changes. Findings are discussed with respect to applications of calcium sulfate-based materials in conservation and rehabilitation interventions.

1. Introduction

Calcium sulfate exists in a variety of hydration states which include gypsum (dihydrate, $CaSO_4{\cdot}2H_2O$), bassanite (Plaster of Paris, hemihydrate, $CaSO_4{\cdot}0.5H_2O$), and anhydrite (anhydrate, $CaSO_4$). Over the course of history, calcium sulfate has been widely used for decorative plasterwork and stucco marble ("scagliola"). Important examples of historic decorative plasterwork include gypsum plaster in the Giza pyramids and adjacent tombs [1] or the "yeseria" of the Alhambra palaces from the Nasrid period (Fig. 1) [2]. Calcium sulfate has also played an important role as a white ground (gesso) for panel paintings and as base for mural paintings [3]. Anhydrite and gypsum-based grounds had a widespread use on Italian and Spanish panel paintings during the thirteenth to sixteenth century [4,5]. Melo et al. [5] reported that often anhydrite was used for the *gesso grosso* (coarse lower layer), while thoroughly slaked burned gypsum was applied as *gesso sottile* (fine upper layer) [4]. In many applications, calcium sulfate was mixed with an organic binder. For example, white ground has been commonly prepared by mixing calcium sulfate (i.e., gypsum and/or anhydrite) with animal glue [4,6–8], and stucco marble is a composite material based on bassanite, animal glue and pigments [3,9]. Rubio Domene [10] suggested that organics such as gelatine, casein, and albumin might have also been added to gypsum used for carved or molded decorative plasterwork ("yeseria") at the Alhambra in order to improve its water resistance. Organic additives have also been used to retard gypsum setting and reduce shrinkage and cracking [9]. Furthermore, it is known that organics affect the gypsum's mechanical strength [9,11–13].

However, investigations on the effect of organic additives [11,13–15] generally focused on industrial applications, and relatively small amounts of organics (≤1 wt%) were added during gypsum hydration in the cited studies. Stucco marble and white grounds, in contrast, contain much larger amounts of organics. Salavessa et al. [9] stated that gypsum-based stucco marble contained ~8 wt% animal glue according to historic recipes and Gettens and Mrose [4] estimated that the gypsum/anhydrite-based ground from a painting by Da Rimini (XIV) contained ~10.5 wt% animal glue. Until now, no comprehensive investigation has been performed on the effect of such large amounts of organic additive on the calcium sulfate's hydration process and mineralogical evolution, which influence significantly the set material's optical and mechanical properties, as well as its weathering resistance. In order to study the organic-inorganic interactions, plaster samples were prepared using commercially available gypsum and alabaster powders with and without the addition of animal glue. Here, rabbit glue was selected because it has been historically used as a common organic binder in calcium sulfate-based composite materials. Despite its widespread historical use, little is known on its effect on gypsum plaster setting as well as on the mechanical and weathering behavior of this material. The latter prevents a complete understanding of this composite material's performance and its

* Corresponding author.
E-mail address: kelert@ugr.es (K. Elert).

https://doi.org/10.1016/j.cemconcomp.2018.12.005
Received 4 September 2018; Received in revised form 5 December 2018; Accepted 11 December 2018
Available online 12 December 2018
0958-9465/

Fig. 1. Example of decorative plasterwork "yeseria" at the Alhambra palaces, Granada, Spain.

optimization for conservation purposes. Samples were subjected to accelerated weathering and mechanical testing, and the obtained results were related to the mineralogical composition and microtextural features. The findings of this study not only assist in the selection of compatible materials for the conservation of decorative plasterwork and painting grounds, but also further the knowledge on calcium sulfate-based composites for general construction purposes.

2. Materials and methods

2.1. Materials and sample preparation/exposure

Three different calcium sulfates and animal glue (rabbit skin glue pearls, No.63028) were purchased from Kremer Pigmente GmbH & Co (Germany) to prepare plaster samples. Table 1 summarizes the manufacturer's data of the calcium sulfates used in this study. Animal glue is a collagen-based binder derived from bones, hides, or fish. It consists of long protein molecules, which are composed of amino acids linked by covalent peptide bonds [16]. Amino acids contain amino and carboxyl functional groups which might form metal-protein complexes [17].

Two sets of samples were prepared for the laboratory studies: (I) For accelerated weathering testing and short-term exposure to high and low RH, plasters were applied to glass slides (Ø 3.3 cm) using a pipette. Plasters were prepared as follows: 7.5 g of animal glue was soaked in 100 g deionized water for 24 h and afterwards heated in a water bath (< 50 °C) under occasional stirring to obtain a homogeneous mixture. After cooling to room *T*, 10 g of aqueous animal glue solution was mixed with 5 g calcium sulfate powder, keeping the organic binder content constant at 15 wt% and the solid/liquid ratio at 0.5:1 by weight. For comparison, powders were mixed with deionized water without the addition of animal glue, maintaining the same solid/liquid ratio as in the case of the animal glue-based plaster samples. Samples were cured under laboratory conditions at 25 °C and 30% RH for 24 h.

(II) For mechanical testing small prisms 5x5x30 mm in size were prepared using plasticine molds. The mixing ratio of gypsum/alabaster powder and water/aqueous animal glue solution was 1:1 by weight with a constant organic binder content of 7.5 wt% (note that the viscosity of higher concentrated glue solution was too high to prepare plaster samples with a mixing ratio of 1:1 by weight). Samples were cured and stored under laboratory conditions (25 °C and 30% RH) for 2 weeks before testing.

The following notation has been used to distinguish the samples: A-B-C; A = mineralogical composition based on semiquantitative X-ray diffraction analysis (A = anhydrite, B = bassanite, G = gypsum, order according to abundance), B = particle size (EF = extrafine, F = fine, M = medium), and C = type of binder (Ag = calcium sulfate mixed with aqueous animal glue solution, H_2O = calcium sulfate mixed with water).

2.2. Laboratory tests

2.2.1. Short-term exposure to < 5% and 100% RH

Once cured, plaster samples (i.e., plaster applied to glass slides) were placed in a tightly closed plastic box for 1 week at 100% and < 5% RH, respectively, in order to determine the effect of animal glue on possible mineralogical changes caused by RH fluctuations. *T* was ~25 °C during testing. The RH was controlled using deionized water and silica gel, and continuously monitored using a SmartReader datalogger (ACR Systems INC. Vancouver, Canada).

2.2.2. Accelerated weathering test (water spray test)

Plaster samples (i.e., plaster applied to glass slides) were attached to a vertical plastic grid with double-sided tape and exposed to repeated spraying (330 ml/sample/day) with deionized water at a distance of 30 cm. Spraying was repeated 7 times over a 3 week period. Water resistance was determined by measuring the material loss over time. Samples were dried under laboratory conditions for 2 days (i.e., until a constant weight was reached) to determine weight loss upon each spraying. Spraying and drying was performed under laboratory conditions (25 °C and 30% RH). Variations in weight due to mineralogical changes during the water spray test (i.e., weight change due to changes in the degree of hydration of calcium sulfate) were considered when calculating weight loss.

2.2.3. Mechanical testing

Tensile and compressive strength were determined using an Instron 3345 (Instron Co., Canton, MA). A load of 50 N (samples prepared with

Table 1
Properties of calcium sulfate powders according to the manufacturer.

Name/Reference/ Authors´ acronym	Denomination/ Provenance	Chemical composition	Particle size (μm)
Alabaster powder/ (No. 58340)/ CS-EF*	Alabaster powder partially calcined/ Lombardy, Italy	$CaSO_4{\cdot}2H_2O$ (gypsum) $CaSO_4{\cdot}0.5\ H_2O$ (bassanite) $CaSO_4$ (anhydrite)	< 75
Terra Alba/ (No. 58300)/ CS-F*	Natural gypsum	$CaSO_4{\cdot}2H_2O$ (gypsum)	< 45
Alabaster plaster/ (No. 58343)/ CS-M*	Alabaster powder partially hydrated	$CaSO_4{\cdot}0.5H_2O$ (bassanite)	99.02% = < 200 85% = < 40

*CS = calcium sulfate, EF = extrafine, F = fine, and M = medium.

water) or 500 N (samples prepared with aqueous animal glue solution) at 1 mm/min was applied for tensile strength measurements. Compressive strength of all samples was measured with a load of 500 N at 3 mm/min. Reported average values are based on 3 (flexural strength) and 6 (compressive strength) measurements per sample.

2.3. Analytical techniques

2.3.1. Particle size analysis (PSA)

The particle size of calcium sulfate powders was measured using a laser particle size analyzer (Mastersizer 2000LF, Malvern Instruments). Powders were dispersed in ethanol.

2.3.2. Chemical analysis

In order to detect possible impurities, chemical analysis of calcium sulfate powders were performed by means of inductively coupled plasma-optical emission spectrometry (ICP-OES, Perkin-Elmer Optima 8300). Note that ICP analysis requires acid digestion in concentrated HCl/HNO_3, resulting in a partial loss of Si, which consequently could not be quantified.

2.3.3. X-ray diffraction (XRD)

The mineralogical composition and mineralogical changes of plaster samples upon laboratory testing were determined using X-ray diffraction (X'Pert PRO PANalytical B.V.). Operational details: Cu-Kα radiation (λ = 1.5405 Å), Ni filter, 45 kV voltage, and 40 mA intensity, 3-60° 2θ exploration range, and 0.05° 2θ s^1 goniometer speed. The identification of mineral phases and semi-quantitative analyses were performed using Xpowder software and experimental RIR (Reference Intensity Ratio) values [18].

2.3.4. Spectrophotometry

Color parameters of plaster samples were measured using a portable spectrophotometer (Minolta CM-700d). Equipment settings were: illuminant D65, 10° observer, Ø 6 mm measurement area. Data were expressed according to CIE L*a*b* color space (i.e., L* is luminosity or lightness (black = 0 and white = 100); a* from +a* (red) to −a* (green), and b* from +b* (yellow) to −b* (blue)). Color changes are reported as ΔL*, Δa*, Δb*, and ΔE. ΔE was calculated using the following formula: $\Delta E = (\Delta L^{*2} + \Delta a^{*2} + \Delta b^{*2})^{½}$. Reported average values are based on a minimum of 5 measurements per sample.

2.3.5. Field emission scanning electron microscopy (FESEM)

Elemental mapping of uncoated plaster samples was performed using a variable pressure FESEM (Supra 40Vp, Carl Zeiss-Germany equipped with an Aztec 3 EDX and X-Max 50 mm detector), working at 40-66 Pa vacuum and 15-20 kV beam accelerating voltage. High-resolution X-ray maps (1024 x 768 pixels) were obtained from selected areas using 100 frames, 10 ms dwell time (2.5 h acquisition time), 3 nA filament current, and 20 eV/ch resolution.

Another FESEM (Auriga, Carl Zeiss, Germany), working at 10^{-4} Pa vacuum and 3 kV in secondary electron imaging mode, was used to study morphological features of powders and plasters. Samples were carbon coated.

2.3.6. Attenuated total reflectance – Fourier transform infrared spectroscopy (ATR-FTIR)

Conformational changes of animal glue were studied using ATR-FTIR spectroscopy (Jasco 6200, JASCO Analytical Instruments, Japan). Small powder samples of plasters and pure binder were analyzed at 2 cm^{-1} resolution over 75 scans from 400 to 4000 cm^{-1}.

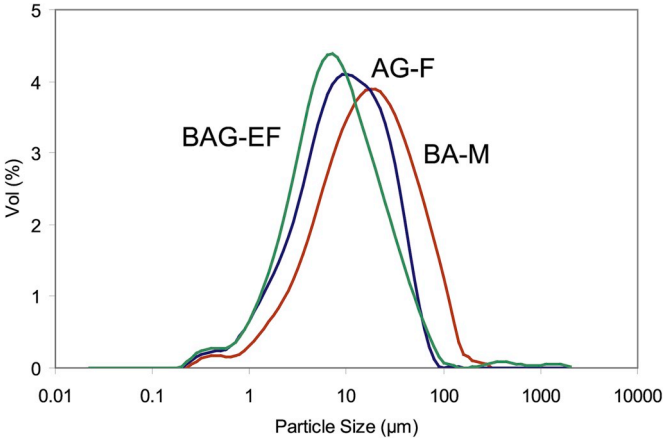

Fig. 2. Particle size distribution of gypsum and alabaster powders. See Table 1 for nomenclature.

3. Results and discussion

3.1. Particle size analysis

Particle size is of great importance as it generally influences the powders surface area and reactivity [19]. All gypsum and alabaster powders showed unimodal particle size distribution with a small contribution of particles < 1 μm (Fig. 2). The principal mode was relatively similar for all calcium sulfate powders, being 7, 9, and 16 μm for BAG-EF, AG-F, and BA-M, respectively. The particle size range was relative wide, being between 0.2 and 85, 0.2–75, and 0.2–160, μm for BAG-EF, AG-F, and BA-M, respectively. Results differed slightly from manufacturer's data (Table 1) reported in the product specification for BAG-EF and AG-F, revealing the presence of a small amount of larger particles in both samples.

3.2. XRD results

3.2.1. Mineralogical composition of calcium sulfate powders

Gypsum is a by-product of several industrial processes (e.g., flue gas desulfurization or phosphoric acid production) or can be produced by grinding of the natural gypsum mineral followed by thermal processing [20]. At elevated *T*, gypsum dehydrates and transforms into β-bassanite (> 100 °C [21]) or γ-anhydrite (100–200 °C, also called anhydrite III [3]) via a topotactic (solid-state) reaction [22]. Note that bassanite exists as α- and β-bassanite, depending on whether it is produced by a wet (i.e., autoclaving) or a dry method (i.e., calcining), respectively [23]. According to Federspiel [24] a mixture of bassanite and γ-anhydrite is obtained when gypsum is heated at standard *T* of 130–160 °C. Upon further heating above ~200 °C, the anhydrite becomes less reactive and it consequently hydrates very slowly in contact with water (i.e., β-anhydrite, also known as anhydrite II or dead burnt gypsum [25]). α- and β-bassanite, in contrast, readily react with water and transform into gypsum (i.e., setting of gypsum) [11]. γ-anhydrite also reacts and sets in contact with water, however, at a slower rate than bassanite [23].

Semiquantitative XRD analysis showed that the purchased gypsum and alabaster powders did not consist of a pure mineral phase but rather a mixture of several calcium sulfate phases with different degrees of hydration, which are indicative of their processing. Note that bassanite and γ-anhydrite can only be differentiated by applying Rietveld refinement [25]. In the following text anhydrite and bassanite refer to β-anhydrite and β-bassanite, respectively, unless indicated otherwise. Overall, the observed mineralogical composition of the analyzed calcium sulfate powders did not always coincide with the manufacturers' information (Table 2). The manufacturer described the extrafine

Table 2
Semiquantitative (± 5 wt%) XRD analysis (wt%) of powders and plaster samples with 15 wt% organic additive used in laboratory studies.

Sample	Mineral phase and JCPDS card number			
	Gypsum 741905	Bassanite 410224	Anhydrite 060226	Dolomite[a] 841208
BAG-EF[b]	3	55	39	3
BAG-EF-Ag[b]	11	56	28	5
BAG-EF-H_2O[b]	90		10	
AG-F[c]	36		64	
AG-F-Ag[c]	57		43	
AG-F-H_2O[c]	53		47	
BA-M		70	26	4
BA-M-Ag	9	67	21	3
BA-M-H_2O	94		6	

[a] Dolomite was only detected in samples containing no or little gypsum. In the remaining samples the 104 dolomite reflection was masked by the 121/002 reflections of gypsum.
[b] Contains trace amounts of quartz.
[c] Contains trace amounts of quartz and calcite.

calcium sulfate (BAG-EF) as partially calcined Italian gypsum, which would contain gypsum and partially or completely dehydrated calcium sulfate phases (Table 1). However, gypsum only amounted to ~3 wt% in this sample and the presence of ~39 wt% anhydrite suggests an extensive calcination at $T > 200$ °C. The presence of anhydrite is not uncommon in commercial products. Seufert et al. [25] reported that dehydrated gypsum at 250 °C contained 3.2 w% bassanite, 73.2 wt% γ-anhydrite, and 23.6 wt% β-anhydrite. Furthermore, small amounts of dolomite and quartz were detected in this sample. Fine calcium sulfate (AG-F) is a "natural ground gypsum" according to the manufacturer. It contained ~64 wt% anhydrite additional to the gypsum claimed by the manufacturer, as well as trace amounts of quartz and calcite. It is unclear whether the high anhydrite content in AG-F is a natural "impurity" (i.e., in natural deposits calcium sulfate commonly occurs as gypsum at shallow depths, while anhydrite is the common phase at greater depths [19] or the result of a partial dehydration of gypsum during processing or storage. The medium sized calcium sulfate (BA-M), a partially hydrated Alabaster powder, did not only contain bassanite as claimed by the manufacturer but also ~26 wt% anhydrite and a small amount of dolomite. Note that carbonates (i.e., calcite and dolomite) and quartz are typical impurities in gypsum deposits [26].

The discrepancy between the manufacturer's information and the actual mineralogical composition of gypsum powders is of great significance, because the calcium sulfate's degree of hydration will condition its water demand as well as volume changes undergone upon hydration (Table 3). Obviously, gypsum will not undergo any further hydration in contact with water. However, some gypsum might dissolve and create crystallization pressure upon reprecipitation according to Charola et al. [27]. Bassanite and anhydrite will experiment an important volume increase upon hydration. Theoretically, the hydration of anhydrite to gypsum is accompanied by a volume increase of 62%, creating a swelling pressure of up to 70 MPa [28]. Nevertheless, according to Bell [28] the actual swelling pressure commonly does not exceed 1–12 Mpa and Singh and Middendorf [21] stated that expansion would be ~1%. This is in contrast to experimental results by Salavessa et al. [9], who reported a volume increase of 9.5% following bassanite hydration in the case of stucco marble containing ~8 wt% animal glue. Overall it can be concluded that some damage due to volume changes might occur, posing a risk in practical applications.

Table 3
Molar volume ($cm^3\ mol^{-1}$) of minerals and calculated theoretical volume change (%) upon phase transition.

Mineral	Molar volume ($cm^3\ mol^{-1}$)	Volume change (%)
Anh	45.8	16.0 (Anh→Bas)
Bas	53.2	39.5 (Bas→Gp)
Gp	74.2	62.0 (Anh→Gp)

Anh = anhydrite, Bas = bassanite, Gp = gypsum.

3.2.2. Mineralogical evolution upon plaster preparation

Generally, it can be expected that hydration of bassanite and/or anhydrite will occur upon mixing with water or an aqueous solution of animal glue and that the gypsum content should increase. However, analytical results revealed that the presence of animal glue drastically inhibited the hydration process and only 5–10 wt% gypsum formed upon plaster preparation in the case of BA-M and BAG-EF (Table 2). Findings regarding delayed hydration are in agreement with previous studies, showing that organics such as carboxylic acids stabilized bassanite and retarded the crystallization of gypsum [17]. When mixed with water, in contrast, hydration was almost complete after 24 h of curing and only 5–10 wt% anhydrite remained. The hydration of bassanite and anhydrite is a solution mediated process [21]. Bassanite is metastable with respect to anhydrite [27], its solubility (8.72 g/L (25 °C)), being higher than that of anhydrite (2.1 g/L (20 °C)) [11]. Actually, it has long been recognized that anhydrite hydrates slowly in contact with water at ordinary T and pressure, especially in the case of larger anhydrite particles [29]. According to Lewry and Williamson [23], anhydrite hydrates via a two-stage reaction to first form bassanite at a relatively low reaction rate, and subsequently gypsum at a higher reaction rate. It is thus not surprising that the hydration of bassanite was complete while not all anhydrite had hydrated in contact with water. Moreover, part of the anhydrite might have been exposed to elevated T (i.e., > 360 °C [25]) during calcination and thus rendered basically unreactive. Experimental results by Farnsworth [29] showed that it took 6 years for dead-burned gypsum to set in contact with water. In the case of plasters prepared with natural gypsum powder (AG-F), extensive hydration of anhydrite was not observed when mixed with water. Possibly, only the fine fraction of the anhydrite in this sample hydrated during plaster preparation, resulting in a 20 wt% decrease of this phase (Table 2).

3.2.3. Mineralogical evolution of plasters during short-term exposure to high and low RH

The short-term exposure for 1 week to extreme high or low RH conditions provoked only minor changes in the plasters' degree of hydration as revealed by XRD, which were within error (± 5 wt%) of this technique (Fig. 3). Furthermore, observed changes did not always follow a logical trend (i.e., the degree of hydration did not always

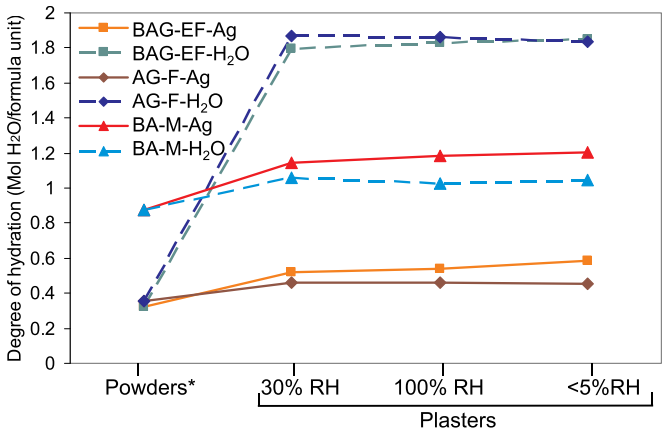

Fig. 3. Degree of hydration based on XRD analysis results of plaster samples exposed at 100% and < 5% RH for 1 week. *The degree of hydration of the original powders and plaster samples cured for 1 day at 30% RH are included for comparison.

Table 4
Semiquantitative (± 5 wt%) XRD analysis (wt%) of plaster samples before (B) and after (A) spraying test.

Sample	Mineral phase and JCPDS card number			
	Gypsum 741905	Bassanite 410224	Anhydrite 060226	Dolomite[a] 841208
BAG-EF-Ag[b] B	11	56	28	5
BAG-EF-Ag[b] A	57	4	39	–
BAG-EF-H_2O[b] B	90	–	10	–
BAG-EF-H_2O[b] A	85	–	15	–
AG-F-Ag[c] B	57	–	43	–
AG-F-Ag[c] A	29	–	71	–
AG-F-H_2O[c] B	53	–	47	–
AG-F-H_2O[c] A	Plaster layer was lost upon spraying			
BA-M-Ag B	9	67	21	3
BA-M-Ag A	4	49	45	2
BA-M-H_2O B	94	–	6	–
BA-M-H_2O A	73	–	27	–

[a] Dolomite was only detected in samples containing no or little gypsum. In the remaining samples the 104 dolomite reflection was masked by the 121/002 reflections of gypsum.
[b] Contains trace amounts of quartz.
[c] Contains trace amounts of quartz and calcite.

decrease during low RH exposure or increase during high RH exposure). It can be concluded that RH fluctuations over short periods of time at room *T* will not significantly affect the degree of hydration of calcium sulfate phases in plasters either in the presence or absence of the organic additive. Remarkably, the bassanite content remained constant in samples BAG-EF-Ag and BA-M-Ag after 1-week exposure at 100% RH, demonstrating that this mineral phase was effectively stabilized in the presence of the organic additive. Note that preliminary XRD results of comparable samples exposed outdoors at the Alhambra palaces revealed that small amounts of bassanite could even be detected after 36 months of exposure in samples which did not suffer direct impact of rain (Table 1 – Supplementary Materials).

3.2.4. Mineralogical evolution of plasters upon accelerated weathering

Unexpectedly, the majority of samples underwent dehydration after 7 weathering cycles (Table 4). Only in the case of BAG-EF-Ag part of the bassanite transformed into gypsum. All other samples suffered a decrease in gypsum and an increase in anhydrite content after repeated wetting and drying. Somewhat puzzling was the difference in the hydration behavior of BAG-EF- and BA-M-based plaster samples (i.e., the latter was more prone to dehydration than the former), which both had initially a similar mineralogical composition (Table 4). The crystallite size of both Alabaster powders, calculated using the Scherrer equation [18], was also quite similar (i.e., 39 nm in the case of BAG-EF and 47 nm in the case of BA-M), and did not justify the observed difference in reactivity. Thus, further research focusing on a detailed characterization (i.e., crystal morphology/strain and presence of impurities) of original powders will be required in order to explain differences in their hydration behavior.

Part of the gypsum transformed into anhydrite upon dehydration in samples with and without organic additive (BAG-EF-H_2O, BA-M-H_2O, and AG-F-Ag). Bassanite as an intermediate phase was not detected. It might be argued that the decrease in gypsum content could be caused by preferential leaching. The solubility of gypsum (2.4 g/L (20 °C) is slightly higher than that of anhydrite (2.1 g/L (20 °C). Furthermore, gypsum dissolution proceeds via first order kinetics, whereas anhydrite dissolution follows the second order equation [30]. However, not all samples suffered a decrease in gypsum content (i.e., gypsum increased by almost 50 wt% in BAG-EF-Ag) despite similar mineralogical composition and identical weathering conditions. Moreover, weight loss upon spraying amounted to ~10 wt% in the case of AG-F-Ag, but the gypsum content decreased by almost 20 wt% in the same sample (Table 4). Thus, the partial transformation of gypsum into anhydrite seems to be the likely cause for the decrease in gypsum concentration upon weathering.

Table 5
Chemical composition (wt%) of calcium sulfate powders.

Sample	Al	Ca	Fe	K	Mg	Mn	Na	S
BAG-EF	0.045	25.07	0.024	1.072	0.861	0.001	1.755	19.39
AG-F	0.271	26.32	0.145	1.261	0.661	0.004	1.812	22.09
BA-M	0.015	27.30	0.013	1.092	0.454	0.001	1.752	21.48

According to data summarized by Van Driessche et al. [20] gypsum dehydration to anhydrite via a dissolution/precipitation process would only occur at $T \geq 38$ °C. In our case, experiments were carried out at 25 °C, and gypsum dissolution and non-equilibrium, kinetically-controlled crystallization of metastable anhydrite seemed to have been facilitated by the high evaporation rate during drying at relative low RH (i.e., 30%) [30]. Sayre [31] already recognized a possible dehydration of gypsum at RH < 35–45% and 24-38 °C. Changes in the degree of hydration are not only of importance in relation with possible paint alteration processes (i.e., possible volume changes during hydration/dehydration) but could also be of significance in the characterization of historic painting materials. Consequently, the reported mineralogical composition of historic gypsum-based samples (e.g., grounds of mediaeval Italian and Spanish paintings [4,32]) might not always reflect the composition of the original materials and could have changed during long-term storage or exhibition depending on the prevailing climate conditions.

3.3. Chemical analysis (ICP-OES)

Chemical analysis revealed the presence of varying amounts of Al and Fe in the analyzed samples (Table 5), which can be related with the presence of aluminosilicates and iron compounds. As mentioned above, Si can not be quantified reliably with this technique, although it was present in BAG-EF and AG-F according to FESEM-EDX (see below). All samples contained significant amounts of Mg due to the presence of dolomite (see XRD and FESEM results below). The above mentioned mineral phases are common impurities in gypsum deposits [26,33,34]. Note that the origin of small amounts of K and Na in all three samples is unknown, but might be related with the presence of impurities such as aluminosilicates and other mineral phases (i.e., double or triple salts such as syngenite, glauberite, and polyhalite) present in the gypsum deposit [22]. The presence of small amounts of impurities (i.e, aluminosilicates and iron compounds) can be related with the observed color variations among the different calcium sulfate powders (see below). Small amounts of dolomite, syngenite, glauberite, and polyhalite, which are all whitish minerals, in contrast, are not thought to have any significant influence on the powders' color.

3.4. Color measurements of calcium sulfate powders and plasters

Color is an important parameter in the case of conservation materials used for example for the reintegration of stucco marble. Measurements revealed minor differences in L* and b* among the various calcium sulfate powders (Table 6). The slightly lower L* value observed for the AG-F sample as compared with the remaining calcium sulfate powders was very likely related to the large amount of gypsum in the former. Harrison [35] reported that gypsum had lower reflectance in the visible wavelength range as compared to bassanite and anhydrite. Variations in b* were most likely associated with impurities, such as clay minerals and iron compounds, which have been detected with ICP-OES and FESEM (see below). Upon mixing with the organic binder all plasters suffered important color changes due to a decrease in luminosity and a shift towards a more yellowish color (i.e., increase in

Table 6
Color measurements of powders and plasters[a] used in laboratory studies.

Sample	L[a]	a[a]	b[a]	ΔL[a]	Δa[a]	Δb[a]	ΔE
BAG-EF	94.59 ± 0.25	1.03 ± 0.08	3.99 ± 0.28				
AG-F	91.56 ± 0.24	0.44 ± 0.01	3.74 ± 0.06				
BA-M	94.64 ± 0.03	0.24 ± 0.01	1.92 ± 0.07				
BAG-EF-Ag	88.60 ± 0.72	1.90 ± 0.13	8.82 ± 0.38	−6.09 ± 0.71	0.87 ± 0.14	4.86 ± 0.39	7.84 ± 0.73
AG-F-Ag	82.38 ± 0.29	1.27 ± 0.03	11.76 ± 0.12	−9.40 ± 0.28	0.83 ± 0.03	8.11 ± 0.12	12.45 ± 0.29
BA-M-Ag	89.75 ± 0.18	0.41 ± 0.01	7.61 ± 0.19	−5.05 ± 0.20	0.16 ± 0.01	5.74 ± 0.19	7.64 ± 0.27
BAG-EF-H_2O	93.05 ± 0.24	1.19 ± 0.03	5.07 ± 0.20	−1.66 ± 0.24	0.16 ± 0.03	1.11 ± 0.20	2.00 ± 0.29
AG-F-H_2O	90.18 ± 0.17	0.48 ± 0.01	4.23 ± 0.08	−1.47 ± 0.18	0.03 ± 0.02	0.52 ± 0.07	1.56 ± 0.19
BA-M-H_2O	93.03 ± 0.11	0.34 ± 0.01	3.07 ± 0.08	−1.76 ± 0.12	0.09 ± 0.01	1.18 ± 0.09	2.12 ± 0.14

[a] Calculated color changes with respect to corresponding powders.

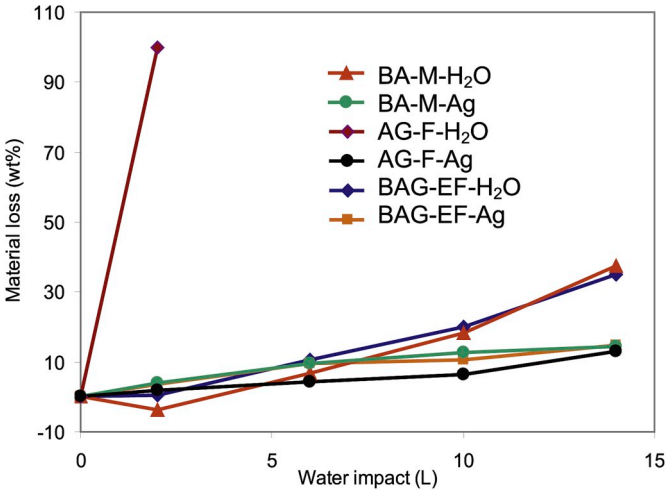

Fig. 4. Weight loss (wt%) of plaster samples upon water spraying.

b*), which was caused by the inherent yellowish color of the animal glue. Mixing with pure water caused only minor color changes below the threshold for human perception [36] as a result of a small decrease in luminosity and a slight increase in b*. Possibly, these changes were related to the gypsum formation after hydration of bassanite and/or anhydrite.

3.5. Accelerated weathering test

According to Sayre [31] gypsum-based materials are more resistant to air pollution-induced decay as compared to lime-based materials. However, gypsum-based plasters are known for their low water resistance, and their use is usually limited to indoor applications [3,37]. The low weathering resistance is related to the gypsum's relatively high solubility (i.e., 2.41 g/L (20 °C)) as compared with calcite (i.e., 0.013 g/L (25 °C)). Nevertheless, our experimental results showed significant differences in water resistance of calcium sulfate-based plaster samples depending on mineralogical composition and presence or absence of organic additive (Fig. 4). Water-based samples generally suffered higher weight loss than corresponding samples prepared with animal glue. Note that the water resistance of BA-M-H_2O and BAG-EF-H_2O is due to gypsum setting (i.e., hydration of anhydrite and bassanite). In the case of the natural gypsum powder (AG-F) only very limited gypsum setting took place according to XRD and the sample was immediately lost upon contact with water. In the presence of animal glue the weight loss of plaster samples was reduced by more than 50% as compared to their water-based counterparts, indicating a substantial improvement in water resistance. Remarkably, sample AG-F-Ag (natural gypsum powder) experienced similar weight loss as the remaining samples containing animal glue, indicating that gypsum setting did not significantly influence the water resistance in samples containing organic binder. The weathering test also revealed an improved adhesion to the glass support of samples prepared with animal glue as compared to purely water-based samples, which detached from their glass supports at an early stage of the test. Gettens and Mrose [4] recognized the need to mix gypsum-based grounds with an organic additive in order to obtain a sufficient bond with the substrate (i.e., wooden or fabric surfaces).

Table 7
Flexural and compressive strength and mineralogical composition of tested plaster samples.

Sample	Flexural strength (MPa)	Compressive strength (MPa)	Mineralogical composition (wt%)[a]	
BAG-EF-H_2O	0.15 ± 0.02	1.02 ± 0.12	Gypsum	83
			Bassanite	Trace
			Anhydrite	17
BAG-EF-Ag	0.53 ± 0.07	1.80 ± 0.47	Gypsum	80
			Bassanite	4
			Anhydrite	16
AG-F-H_2O	0.04 ± 0.01	0.22 ± 0.05	Gypsum	42
			Anhydrite	58
AG-F-Ag		Not available[b]		
BA-M-H_2O	0.14 ± 0.02	0.93 ± 0.33	Gypsum	79
			Bassanite	Trace
			Anhydrite	21
BA-M-Ag	0.37 ± 0.10	1.40 ± 0.57	Gypsum	40
			Bassanite	32
			Anhydrite	28

[a] Based on semiquantitative (± 5 wt%) XRD analysis.
[b] It was impossible to obtain a coherent/intact prismatic sample using the same water/solid mixing ratio as used for the remaining samples.

3.6. Mechanical strength

The flexural and compressive strength of all samples was below the minimum requirements (i.e., bending strength ≥1 MPa and compressive strength ≥2 MPa [38]) established for gypsum binders and gypsum plasters (Table 7). They were also significantly lower than most reported values for gypsum mortars [12,39]. The microstructure of gypsum pastes influences physical and engineering properties [21], and it is known that porosity is a determining factor in controlling strength. The porosity of the final material is greatly influenced by the water/gypsum mass ratio, which commonly is 0.6–0.8 [40,41]. Possibly, the high water/gypsum mass ratio (i.e., 1.0) of our samples resulted in a fairly porous material of relative low strength [13,40]. Furthermore, the delayed hydration of anhydrite, present in the original powders, might have contributed to the low mechanical strength. As mentioned above, the hydration of anhydrite proceeds in a two-stage reaction and the newly formed hydration products might have disrupted the interlocked crystal matrix originally formed during the hydration of bassanite [23].

In the case of samples mixed with water, important differences in strength development were observed depending on their mineralogical

composition. It was not surprising that flexural and compressive strength of natural gypsum powder (AG-F-H_2O) was extremely low, because hardly any setting occurred upon mixing with water (Table 7). Samples BAG-EF-H_2O and BA-M-H_2O, in contrast, revealed higher strength due to extensive gypsum formation (Table 7). Both showed similar flexural and compressive strength, which is in agreement with their almost identical mineralogical composition and morphological features (see FESEM results below).

Generally, mechanical strength increased significantly when the calcium sulfate powders were mixed with aqueous animal glue solution instead of water, especially in the case of the flexural strength, which increased by more than 100%. The observed compressive strength values of animal glue-based samples were actually similar to that reported for gypsum-based stucco marble containing ~8 wt% animal glue [9]. Our results further showed that strength was not only controlled by the organic binder and that mineralogical changes during gypsum setting were also influential (i.e., BAG-EF-Ag contained ~40 wt% more gypsum and showed 30% and 22% higher flexural and compressive strength, respectively, as compared to BA-M-Ag (Table 7)). Frequently, it has been reported that the gypsum's strength decreased in the presence of small amounts (≤1 wt%) of organic additives as a result of their inhibiting/retarding effect on gypsum setting and modifications of the gypsum's microstructure [12,14,21]. Our data indicate that in binary systems with relatively high organic binder content (7.5 wt%), a strength increase was observed if compared to water-based samples. Furthermore, calcium sulfate powders did not only act as fillers and gypsum setting also contributed to the final strength of the composite material.

Improved strength, especially flexural strength, might at least in part counteract damage created by climate-induced dimensional changes of the substrate (e.g., wood in the case of panel paintings or stuccos), which can lead to buckling, cracking, and loss of the gypsum layer [42]. However, it has to be kept in mind that animal glue is a very hygroscopic material. According to Karpowicz [43] the moisture content of animal glue increases drastically at ≥30% RH and might reach 30–50 wt%, leading to dimensional changes due to swelling [44]. Therefore, the optimal animal glue content for grounds and decorative plasters has to be established, which would allow for sufficient mechanical strength improvement without creating an overly hygroscopic material with a strong and deleterious response to climate fluctuations [44].

3.7. FESEM analysis of calcium sulfate powders and plasters

Elemental mapping corroborated ICP-OES results, revealing the presence of mainly Ca and S, together with small amounts of Mg, Si, Al, K, and Fe in AG-F-Ag and BAG-EF-Ag, confirming the presence of impurities such as dolomite (Mg), quartz (Si), aluminosilicates such as clay minerals or feldspars (Mg, Si, Al, K, Fe), and iron oxyhydroxides (Fe). In BA-M-Ag, in contrast, only Ca, S, and Mg could be detected with this technique. As mentioned above, aluminosilicates and iron oxyhydroxides can be held responsible for the color variations detected among the studied calcium sulfate powders, causing a slightly more reddish/yellowish color in AG-F and BAG-EF-based plasters (Table 6). Note that Mg, Si, and Al are common impurities, which have also been identified in historic gypsum-based grounds of mediaeval Italian and Spanish paintings [4].

FESEM micrographs showed distinct morphological features of calcium sulfate powders, which depended on their mineralogical composition. Powders containing bassanite and anhydrite (i.e., BAG-EF and BA-M, Fig. 5a and c) were formed by aggregates of randomly oriented, mainly nano-sized particles. Aggregates were generally smaller in BAG-EF (i.e., principal mode at 7 μm according to PSA, Fig. 2), as compared with BA-M (i.e., principal mode at 16 μm). The natural ground gypsum, containing gypsum and anhydrite (AG-F with principal mode at 9 μm), in contrast, was made up of blocky crystals with irregular edges/fractured appearance, typical for powders obtained by grinding bigger lumps (Fig. 5).

Important morphological changes were detected in BAG-EF and BA-M upon mixing with water (Fig. 5d and f), which provoked the precipitation of gypsum crystals with typical needle and rod-shape habits [11], forming an interlocked structure. This is in agreement with the mineralogical changes (i.e., extensive gypsum formation) observed in these samples (Table 2). In AG-F-H_2O, in contrast, only very limited morphological changes were detected, indicated by a very small amount of short rod-like gypsum crystals, which did not produce the typical interlocked structure (Fig. 5e). This finding is in agreement with XRD results, showing an increase in gypsum content of only ~20 wt% in the later sample (Table 2). These morphological features also explain the sample's exceptionally low flexural and compressive strength (Table 7). According to Amathieu and Boistelle [11] mechanical properties are significantly influenced by the size and shape of particles, the area of contact between the crystals, their degree of interlocking, and the bond strength. Generally, strength development can be related with the formation of an interlocked structure by needle-shaped gypsum crystals [23].

The presence of animal glue inhibited morphological changes to a large extent in all samples. The aggregates comprised of nano-sized particles in BAG-EF-Ag and BA-M-Ag were surrounded by the organic binder and seemed to have disintegrated into smaller aggregates in the case of the later sample (Fig. 5g and i). Rod-like gypsum crystals were not detected in either of the two samples. In AG-F-Ag particles were partially covered by animal glue and significant morphological changes could not be detected (Fig. 5h). These observations are in agreement with XRD results, revealing only minor mineralogical transformations (Table 2). Commonly, the formation of Ca-organic complexes is held responsible for the stabilization of bassanite and the retardation of gypsum precipitation in gypsum-based materials with low (i.e., ≤1 wt %) organic additive content [17,45]. In our case, the large amount of animal glue seemed to have acted as a physical barrier, impeding the dissolution of bassanite and anhydrite during plaster setting. Furthermore, the water activity was reduced in the presence of animal glue, which also hindered the dissolution and hydration of bassanite and anhydrite and led to their stabilization. Evidence for the formation of Ca-organic complexes, in contrast, was not observed in the unweathered plasters (see ATR-FTIR below).

Morphological changes observed upon accelerated weathering were in general agreement with compositional changes detected with XRD (Table 4).. Sample BAG-EF-H_2O did not suffer either morphological or important mineralogical changes, still revealing mainly needle or rod-shape crystals typical for gypsum (Fig. 6a). In the weathered BA-M-Ag sample, in contrast, a significant amount of small crystals (2–3 μm in size) were observed, which seems to be related with the ~25 wt% increase in anhydrite (arrow, Fig. 6b). Likely, this morphological change will affect the sample's mechanical properties negatively. BAG-EF-Ag also underwent morphological changes and a few isolated hexagonal plate-like crystals were detected, which suggest the formation of an organic-inorganic hybrid material in this weathered plaster (Fig. 6c). Possibly, the repeated wetting of the plaster sample facilitated an organic-inorganic interaction and the organic additive was preferentially adsorbed on the (111) faces of newly formed gypsum crystals, slowing down their growth rate and yielding wider plate-like crystals [45,46]. According to Barcelona and Atwood [45] the (111) face is populated by calcium ions, which facilitate the formation of Ca-organic complexes. Amathieu and Boistelle [11] reported on the formation of similar gypsum crystals in the presence of organic additives (i.e., nitrilotrimethylene phosphonic acid or diethylene triansine pentaacetic acid), which slowed the setting kinetics and produced a very friable plaster. AG-F-Ag and BA-M-Ag did not reveal any significant morphological changes (Fig. 6d), even though the anhydrite content increased by > 20 wt% in both samples upon weathering. However, the originally large aggregates in the later sample partially disaggregated (Fig. 6e).

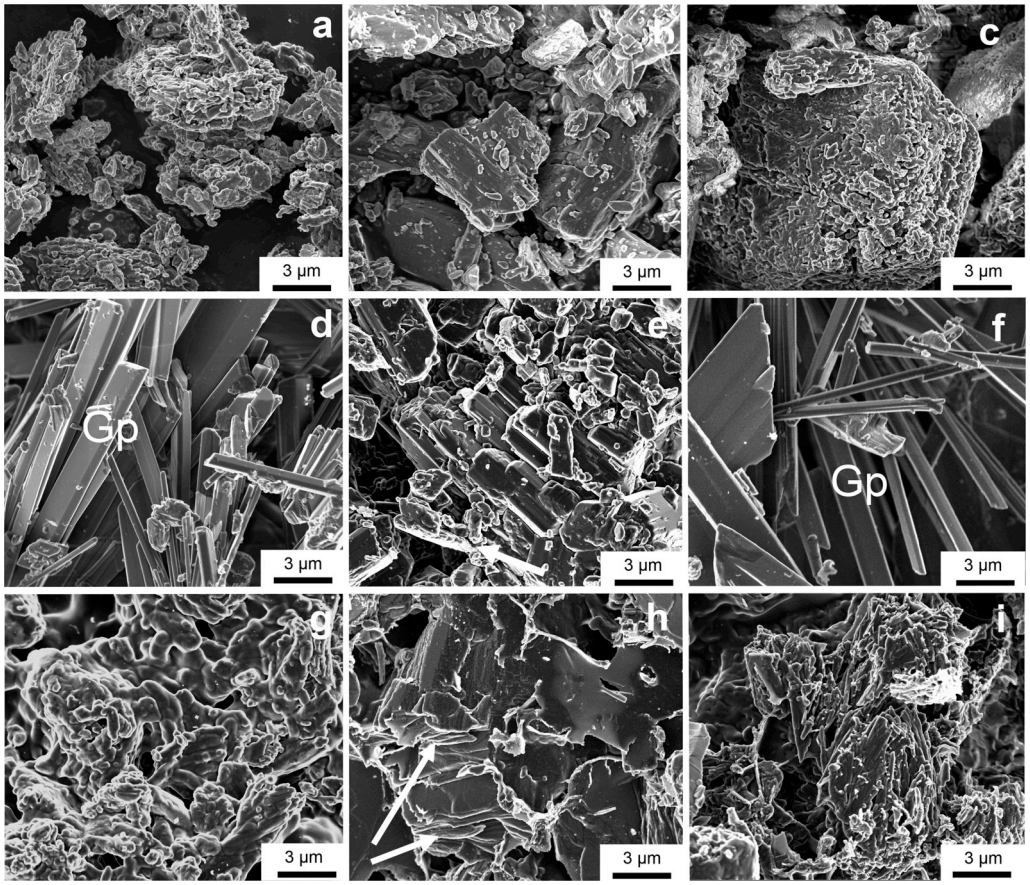

Fig. 5. FESEM micrographs of powders: a) BAG-EF, b) AG-F, and c) BA-M; water-based plasters before weathering: d) BAG-EF-H_2O, e) AG-F-H_2O, and f) BA-M-H_2O; animal glue-based plasters before weathering: g) BAG-EF-Ag, h) AG-F-Ag, arrow indicates particle delamination, and i) BA-M-Ag.

Overall, FESEM observation confirmed XRD results, evidencing morphological changes compatible with important dehydration (i.e., gypsum to anhydrite transformation) upon accelerated weathering.

3.8. ATR-FTIR analysis of plasters

Using ATR-FTIR no evidence for the formation of Ca-organic complexes was obtained (Fig. 7). Commonly, the formation of metal-protein complexes are accompanied by a blue shift of the protein's amide I band (carbonyl stretching), indicating a reduction in hydrogen bonds-between N—H and C═O groups of protein chains [47,48]. In the presence of different metal compounds, protein chains undergo important conformational changes from β-sheet to random coil, offering sites (i.e., carboxyl groups) for the formation of metal-protein complexes [49]. In the case of calcium sulfate powders mixed with animal glue only a small red shift from 1625 to 1620 cm^{-1} was observed in the amide I band,

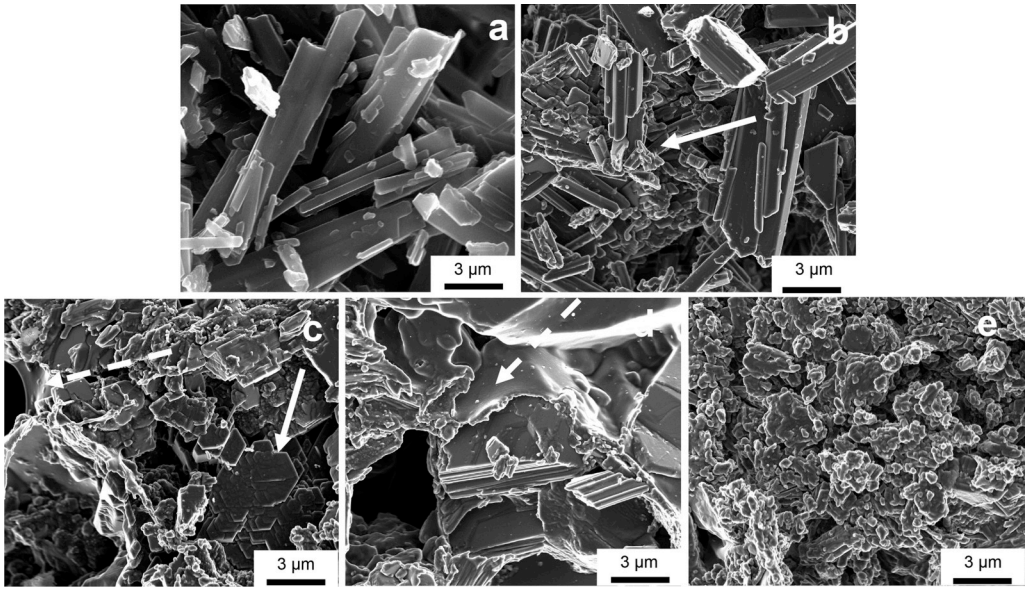

Fig. 6. FESEM micrographs of water-based plasters after accelerated weathering: a) BAG-EF-H_2O and b) BA-M-H_2O, arrow showing newly formed small crystals; and animal glue-based plasters after accelerated weathering:c) BAG-EF-Ag showing plate-like gypsum crystals (arrow) and animal glue (dashed arrow), d) AG-F-Ag, dashed arrow showing animal glue film, and e) BA-M-Ag.

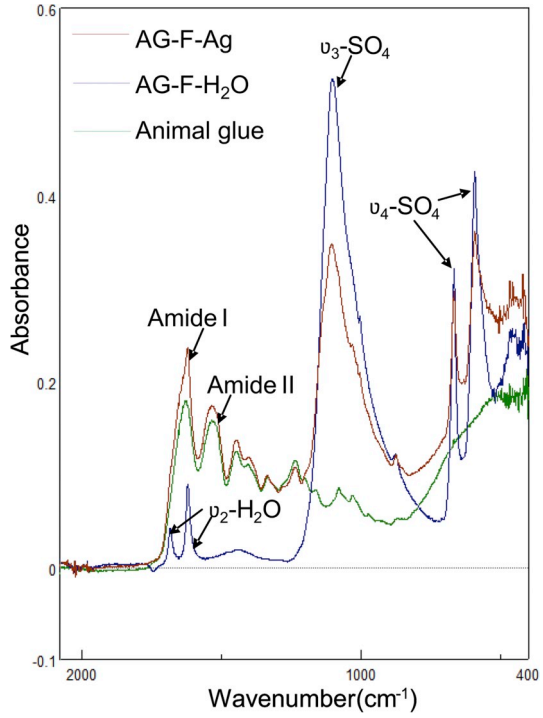

Fig. 7. ATR-FTIR spectra of cured plasters and pure animal glue.

suggesting that the organic binder did not undergo any significant conformational changes and remained as a β-sheet structure, making the formation of metal-protein complexes unlikely. The position of the amide II band (N-H bending) remained unchanged. At near neutral pH (i.e., freshly prepared calcium sulfate pastes have a pH of ~8) only the carboxyl group is negatively charged and could form Ca-organic complexes, whereas the amino group is either uncharged or positively charged and will not likely form complexes with Ca^{2+} [17,50]. These results support the hypothesis that significant complexation did not take place in unweathered plasters and that the observed stabilization of bassanite and anhydrite in the presence of animal glue was due to the formation of a physical barrier and a reduction in water activity, both hindering the dissolution and hydration of bassanite and anhydrite.

4. Conclusion

Mineralogical analyses revealed that commercial calcium sulfate-based powders consisted of a mixture of different calcium sulfate phases with varying degree of hydration. Their composition differed in some cases from manufacturer's data. These results demonstrate the necessity to perform a detailed mineralogical analysis before their use in conservation interventions or scientific investigations, because the degree of hydration will condition the calcium sulfates' water demand and volume expansion during plaster preparation.

Color measurements showed that the mineralogical composition as well as small amounts of impurities (i.e., aluminosilicates and iron compounds) influenced the color of calcium sulfate-based powders. However, the organic binder had an even greater effect on the plaster's final color and has to be taken into consideration when plasters are used for the reintegration of original stuccos.

The presence of animal glue affected the mineralogical composition of calcium sulfate-based plasters by stabilizing metastable bassanite as well as anhydrite over a 36-month period and inhibiting gypsum formation significantly. Analytical results suggest that animal glue acted as a barrier and reduced the water activity, thus hindering dissolution and facilitating the stabilization of bassanite and anhydrite. Possible evidence for the formation of metal-protein complexes (i.e., organic-induced habit modification leading to the formation of hexagonal gypsum crystals) was only observed in the case of one plaster sample exposed to accelerated weathering by repeated water spraying. Upon accelerated weathering changes in the degree of hydration of calcium sulfate were observed in almost all samples. The associated phase transformations caused morphological changes, which likely induce volumetric changes. These changes could affect the plasters' strength negatively and accelerate deterioration. These climate-induced phase changes should also be considered in the study of historic plasters and painting grounds, where the original composition might have changed depending on the prevailing climate conditions upon long-term storage or exhibition. Even though, water resistance of gypsum-based materials was improved in the presence of animal glue, these composite materials will not likely survive the direct impact of rain over a long period of time. In order to obtain a more water resistant material, animal glue could be replaced by a less water soluble organic binder such as casein, egg yolk or a synthetic polymer. However, possible phase changes upon periodic wetting and subsequent drying have to be considered, limiting the outdoor application of gypsum-based plasters to areas where they are protected from the direct impact of rain or condensation.

Calcium sulfate-based materials showed differences in mechanical strength, which were controlled by the mineralogical composition, its evolution upon hydration, and the presence or absence of organic binder. These results indicate that plasters and painting grounds could be prepared according to the strength requirements of each particular application. By varying organic binder and mineral phase concentration (i.e., content of anhydrite, bassanite, and gypsum) as well as the water/calcium sulfate mixing ratio, materials with an even wider range of mechanical properties could be obtained. However, very high organic binder concentrations are not recommended because they could lead to a highly hygroscopic composite material, which could undergo drastic dimensional changes and lose structural stability at high RH. In addition, very high binder concentrations could also cause more significant color changes due to photo-induced yellowing of the organic additive (i.e., animal glue) and increase the susceptibility for biodeterioration. Future research should address the possible risk of deterioration by microorganisms of such organic-inorganic composite materials.

Acknowledgement

This research was financed by the Spanish Research Projects AERIMPACT (CGL2012-30729) and EXPOAIR (P12-FQM-1889), the European Regional Development Fund, and the Junta de Andalucía. FESEM analyses were performed at the Centro de Instrumentación Científico (UGR). K. Elert is a post-doctoral fellow in the EXPOAIR Project. We are grateful to C. Rodriguez-Navarro for comments and suggestions and thank A. Herrera Rubia for assistance with long-term outdoor exposure tests.

Appendix A. Supplementary data

Supplementary data to this article can be found online at https://doi.org/10.1016/j.cemconcomp.2018.12.005.

References

[1] A. Lucas, J. Harris, Ancient Egyptian Materials and Industries, Dover Publications Inc., Mineola (New York), 2012.
[2] C. Cardell-Fernández, C. Navarrete-Aguilera, Pigment and plasterwork analyses of Nasrid polychromed lacework stucco in the Alhambra (Granada, Spain), Stud. Conserv. 51 (2006) 161–176.
[3] C. Rodríguez-Navarro, Binders in historical buildings: traditional lime in conservation, Seminarios de la Sociedad Española de Mineralogía (SEM) 9 (2012) 91–112.
[4] R.J. Gettens, M.E. Mrose, Calcium sulphate minerals in the grounds of Italian paintings, Stud. Conserv. 1 (1954) 174–189.
[5] H.P. Melo, A.J. Cruz, A. Candeias, J. Mirão, A.M. Cardoso, M.J. Oliveira, S. Valadas, Problems of analysis by FTIR of calcium sulphate–based preparatory layers: the case

of a group of 16th-century Portuguese paintings, Archaeometry 56 (2014) 513–526.
[6] C. Cennini, El libro del Arte, AKAL S.L., Madrid, 1988.
[7] V. Antunes, A. Candeias, M.J. Oliveira, S. Longelin, V. Serrão, A.L. Seruya, J. Coroado, L. Dias, J. Mirão, M.L. Carvalho, Characterization of gypsum and anhydrite ground layers in 15th and 16th centuries Portuguese paintings by Ramon spectroscopy and other techniques, J. Raman Spectrosc. 45 (2014) 1026–1033.
[8] J. Romero-Pastor, A. Duran, A.B. Rodríguez-Navarro, R. Van Grieken, C. Cardell, Compositional and quantitative microtextural characterization of historic paintings by micro-X-ray diffraction and Raman microscopy, Anal. Chem. 83 (2011) 8420–8428.
[9] E. Salavessa, S. Jalali, L.M.O. Sousa, L. Fernandes, A.M. Duarte, Historical plasterwork techniques inspire new formulations, Constr. Build. Mater. 48 (2013) 858–867.
[10] R. Rubio Domene, Yeserías de la Alhambra, historia, técnica y conservación, Editorial Universidad de Granada, Spain, 2010.
[11] L. Amathieu, R. Boistelle, Improvement of the mechanical properties of set plasters by means of four organic additives inducing {1O1} faces, J. Cryst. Growth 79 (1986) 169–177.
[12] M. Singh, M. Garg, Retarding action of various chemicals on setting and hardening characteristics of gypsum plaster at different pH, Cement Concr. Res. 27 (1997) 947–950.
[13] H.C. Wu, Y.M. Xia, X.Y. Hu, X. Liu, Improvement on mechanical strength and water absorption of gypsum modeling material with synthetic polymers, Ceram. Int. 40 (2014) 14899–14906.
[14] M. Lanzón, P.A. García-Ruiz, Effect of citric acid on setting inhibition and mechanical properties of gypsum building plasters, Constr. Build. Mater. 28 (2012) 506–511.
[15] P.P. Zhou, H.C. Wu, Y.M. Xia, Influence of synthetic polymers on the mechanical properties of hardened β-calcium sulfate hemihydrate plasters, J. Ind. Eng. Chem. 33 (2016) 355–361.
[16] N.C. Schellmann, Animal glues: a review of their key properties relevant to conservation, Stud. Conserv. 52 (sup1) (2007) 55–66.
[17] P. Tartaj, J. Morales, L. Fernández-Díaz, $CaSO_4$ Mineralization in carboxy-and amino-functionalized reverse micelles unravels shape-dependent transformations and long-term stabilization pathways for poorly hydrated nanophases (bassanite), Cryst. Growth Des. 15 (2015) 2809–2816.
[18] J.D. Martín-Ramos, Using XPowder: a Software Package for Powder X-ray Diffraction Analysis, (2004) (GR 1001/04. ISBN 84-609-1497-6.
[19] A. Klimchouk, The dissolution and conversion of gypsum and anhydrite, Int. J. Speleol. (Edizione Italiana) 25 (1996) 2.
[20] A.E. Van Driessche, T.M. Stawski, L.G. Benning, M. Kellermeier, Calcium sulfate precipitation throughout its phase diagram, in: A.E. Van Driessche, M. Kellermeier, L.G. Benning, D. Gebauer (Eds.), New Perspectives on Mineral Nucleation and Growth, Springer, Switzerland, 2017, pp. 227–256.
[21] N.B. Singh, B. Middendorf, Calcium sulphate hemihydrate hydration leading to gypsum crystallization, Prog. Cryst. Growth Char. Mater. 53 (2007) 57–77.
[22] D. Freyer, W. Voigt, Crystallization and phase stability of $CaSO_4$ and $CaSO_4$–based salts, Monatsh. Chem. 134 (2003) 693–719.
[23] A.J. Lewry, J. Williamson, The setting of gypsum plaster: part III-The effect of additives and impurities, J. Mater.Sci 29 (1994) 6085–6090.
[24] B. Federspiel, Questions about medieval gesso grounds, in: A. Wallert, E. Hermens, M. Peek (Eds.), Historical Painting Techniques, Materials, and Studio Practice, J.Paul Getty Trust, Los Angeles, 1995, pp. 58–64.
[25] S. Seufert, C. Hesse, F. Goetz-Neunhoeffer, J. Neubauer, Quantitative determination of anhydrite III from dehydrated gypsum by XRD, Cement Concr. Res. 39 (2009) 936–941.
[26] R. Sharpe, G. Cork, Gypsum and anhydrite, in: J.E. Kogel, N.C. Trivedi, J.M. Barker, S.T. Krukowski (Eds.), Industrial Minerals & Rocks, Littletown, Society for Mining, Metallurgy, and Exploration, Inc, 2006, pp. 519–540.
[27] A.E. Charola, J. Pühringer, M. Steiger, Gypsum: a review of its role in the deterioration of building materials, Environ. Geol. 52 (2007) 339–352.
[28] F.G. Bell, Natural hazards and the environment, in: B. De Vivo, B. Grasemann, K. Stüwe (Eds.), Geology, vol. V, Eolss Publishers Co. Ltd, Oxford, 2009, pp. 160–223.
[29] M. Farnsworth, The hydration of anhydrite, Ind. Eng. Chem. 17 (1925) 967–970.
[30] C. Rodriguez-Navarro, E. Doehne, E. Sebastian, How does sodium sulfate crystallize? Implications for the decay and testing of building materials, Cement Concr. Res. 30 (2000) 1527–1534.
[31] E.V. Sayre, Deterioration and restoration of plaster, concrete and mortar, in: S. Timmons (Ed.), Preservation and Conservation: Principles and Practices, Preservation Press, National Trust for Historic Preservation in the United States, Washington, 1976, pp. 191–201.
[32] R.J. Gettens, G.L. Stout, Painting Materials: a Short Encyclopaedia, Dover Publications Inc, New York, 1966.
[33] W.A. Deer, R.A. Howie, J. Zussman, Rock-forming Minerals vol. 5, Longmans, London, 1962.
[34] R.C. Murray, Origin and diagenesis of gypsum and anhydrite, J. Sediment. Res. 34 (1964) 512–523.
[35] T.N. Harrison, Experimental VNIR reflectance spectroscopy of gypsum dehydration: investigating the gypsum to bassanite transition, Am. Mineral. 97 (2012) 598–609.
[36] R.S. Berns, Principles of Color Technology, third ed., Wiley-Blackwell, Hoboken, 2000.
[37] B. Middendorf, Physico-mechanical and microstructural characteristics of historic and restoration mortars based on gypsum: current knowledge and perspective, Geol Soc London Spec Publ 205 (2002) 165–176.
[38] EN 13279-1, Gypsum Binders and Gypsum Plasters. Part 1: Definitions and Requirements, European Committee for Standardization (CEN), 2008 2008.
[39] J. Karni, E.Y. Karni, Gypsum in construction: origin and properties, Mater. Struct. 28 (1995) 92–100.
[40] P. Padevet, P. Tesárek, T. Plachý, Evolution of mechanical properties of gypsum in time, Intern J Mechan 5 (2011) 1–9.
[41] J. Adrien, S. Meille, S. Tadier, E. Maire, L. Sasaki, In-situ X-ray tomographic monitoring of gypsum plaster setting, Cement Concr. Res. 82 (2016) 107–116.
[42] M.F. Mecklenburg, C.S. Tumosa, D. Erhardt, Structural response of painted wood surfaces to changes in ambient relative humidity, in: V. Dorge, F.C. Howlett (Eds.), Painted Wood: History and Conservation, The Getty Conservation Institute, Los Angeles, 1998, pp. 464–483.
[43] A. Karpowicz, Ageing and deterioration of proteinaceous media, Stud. Conserv. 26 (1981) 153–160.
[44] M.J. Richard, M.F. Mecklenburg, C.S. Tumosa, Technical considerations for the transport of panel paintings, in: K. Dardes, A. Rothe (Eds.), The Structural Conservation of Panel Paintings, Los Angeles: the J.P, Getty Trust, 1998, pp. 525–556.
[45] M.J. Barcelona, D.K. Atwood, Gypsum-organic interactions in natural seawater: effect of organics on precipitation kinetics and crystal morphology, Mar. Chem. 6 (1978) 99–115.
[46] A.M. Cody, R.D. Cody, Chiral habit modifications of gypsum from epitaxial-like adsorption of stereospecific growth inhibitors, J. Cryst. Growth 113 (1991) 508–519.
[47] C. Cardell, A. Herrera, I. Guerra, N. Navas, L.R. Simón, K. Elert, Pigment-size effect on the physico-chemical behavior of azurite-tempera dosimeters upon natural and accelerated photo aging, Dyes Pigments 141 (2017) 53–65.
[48] K. Elert, A. Herrera, C. Cardell, Pigment-binder interactions in calcium-based tempera paints, Dyes Pigments 148 (2018) 236–248 2018.
[49] J. Kong, S. Yu, Fourier Transform infrared spectroscopic analysis of protein secondary structures, Acta Biochim. Biophys. Sin. 39 (2007) 549e59.
[50] S. Fox, I. Büsching, W. Barklage, H. Strasdeit, Coordination of biologically important a-amino acids to calcium(II) at high pH: insights from crystal structures of calcium a-aminocarboxylates, Inorg. Chem. 46 (2007) 818e24.